PROCEEDINGS OF SCIENCE

Operation of CMS GE1/1 GEM detectors in Run-3

S. Calzaferri, on behalf of the CMS Collaboration[a,*]

[a] *Università degli Studi di Pavia, Via Bassi, 6, Pavia, Italy*

E-mail: simone.calzaferri@cern.ch

The muon system of the CMS experiment at the LHC has been upgraded by the installation of the first station of Gas Electron Multiplier (GEM), GE1/1, over the Long Shutdown (LS) 2. The High-Luminosity phase of the LHC (HL-LHC) upgrade for CMS incorporates two additional stations, GE2/1 and ME0. Three GE2/1 chambers have been installed in CMS, with two new ones added at the beginning of 2024, while ME0 is slated for installation during LS3. The aim is to enhance the muon system's capabilities for HL-LHC by extending its acceptance up to $|\eta| = 2.8$ and improving the muon triggering while maintaining performance achieved during Run 2. We present operational aspects of GEM detectors during Run 3, covering detector stability and performance metrics such as muon detection efficiency. Finally, we report on the effects of magnetic field variations observed during commissioning and address the correlation between GEM baseline currents and LHC beam luminosity.

42nd International Conference on High Energy Physics (ICHEP2024)
18-24 July 2024
Prague, Czech Republic

*Speaker

PoS(ICHEP2024)896

1. The GE1/1 detectors

During LS2, the CMS experiment [1, 2] has been upgraded installing 144 triple-GEM modules, composing the GE1/1 station. These detectors cover the pseudorapidity region $1.55 < |\eta| < 2.18$. In each of the two endcaps of CMS 72 modules are installed, organized in pairs. Each pair of modules installed in a given ϕ sector defines a Super-Chamber, with the module closer to the interaction point called Layer-1, while the farther is called Layer-2. The gas mixture adopted for operations of GE1/1 in CMS is Ar/CO_2 (70/30).

The basis element of the GEM detector is the GEM foil, which is a polyimide foil (50 μm thick) and copper cladded on both sides [3]. Biconical holes are etched on the foil (70 μm of diameter) with a pitch of 140 μm. Thanks to this design, the GEM foil can generate an intense electric field ($\sim$ 80 kV/cm) inside the GEM foil holes, when a modest potential difference is applied between the two faces of the GEM foil ($\sim 400\,V$). This intense electric field is achieved for a multiplication of electrons entering the hole.

The multiplication of the primary ionization electrons generated by a ionising particle crossing the gas medium in GE1/1 is achieved in three stages, by stacking three GEM foils one above the other. A schematic drawing of the GEM stack is represented in Figure 1 and more details on the GE1/1 design can be found in [4].

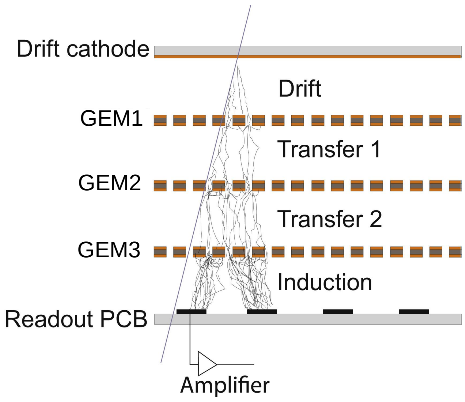

Figure 1: Schematic representation of a triple GEM detector.

2. The High Voltage system

To multiply the primary ionization charge, High Voltage (HV) needs to be provided to the detector. The proportions of the voltages set to power each pair of surfaces in the GEM stack are defined by a resistive divider illustrated in [5], with a total resistance of 4.7 $M\Omega$.

Once installed in CMS the HV divider is replaced by an A1515BTG power supply [6], which offer the flexibility of varying the voltage of each electrode in the stack. Instead of specifying all the seven voltages needed to power the detector stack, the current I_{eq} flowing in the reference resistive divider can be used to identify this set with a unique number: three channels of the board are used to provide the HV between the two faces of each GEM foil, while other four channels provide the HV to the gas gaps [7].

As with other Micro Patter Gas Detectors, GEM detectors are subject to the occurrence of discharges. To limit the amount of energy deposition by individual discharges, in order to prevent potential damage to the foils, the top face of GE1/1 GEM foils have been segmented in sectors, all with an area of around ~ 100 cm^2. The circuit to provide HV from the power supply to each HV sector is represented in Figure 2.

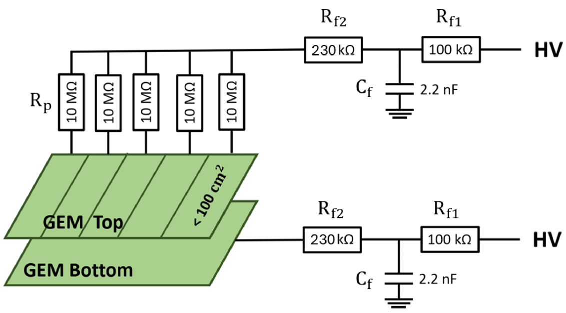

Figure 2: Schematic representation of HV from the power supply to each HV sector of a GEM foil in a GE1/1 detector.

3. Operation of GE1/1 detectors in presence of LHC beam

From July 2022 GE1/1 detectors were operated for the first time in presence of the LHC beam. One plot of the current seen on the power supply channel powering one GEM foil is represented in Figure 3. In the figure there is a baseline current proportional to the instantaneous luminosity of the LHC beams collisions, and current spikes on top of it, identifying the discharges. The occurrences of discharge proved to be challenging in the first months of Run-3, but finally the rate stabilized at ~ 1 $discharge/hour$ per detector by operating the detectors with an HV voltage configuration corresponding to $I_{eq} = 690\,\mu$A.

Preliminary studies indicate that the discharge rate is a linear function of the luminosity of LHC beam collisions. This is shown in Figure 4. This dependence needs to be studied in terms of the I_{eq} adopted for each detector, in the cases the detector is operating above, on, or below the optimal HV working point.

4. Short circuits in GEM foils

During the operation of the GE1/1 detector occurrences of short circuits were observed in the GEM foils. Thanks to the segmentation of the top face of the GEM foil, only one HV sector of the GEM foil gets deactivated and the unaffected ones can still be used for primary electron multiplication. The presence of the short circuit generates a current flowing inside the resistors in the distribution circuit illustrated in Figure 2.

In some cases it was observed the recovery (“healing”) of short circuits: by a sudden drop of the current to 0 μA, or by a slow process of reduction of the current drained by the short circuit (we

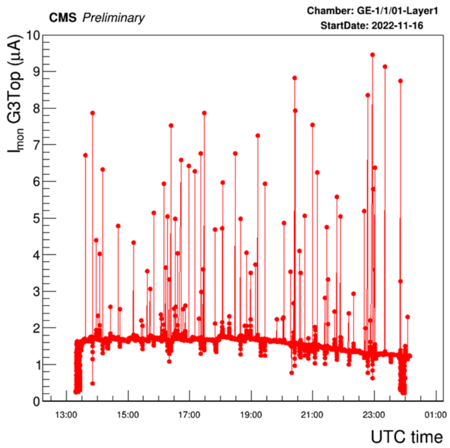

Figure 3: Current observed on the HV channel powering GEM3 foil in presence of LHC beam collisions [8].

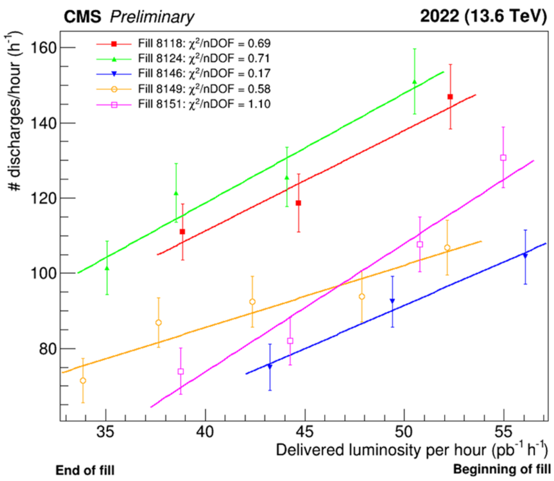

Figure 4: Average discharge rate produced by 143 chambers during LHC beam collisions in 2022. The detectors were powered with an HV configuration equivalent to $I_{eq} = 690\,\mu$A. It can be noticed as the discharge rate is higher for a higher luminosity, corresponding to the time at the beginning of the LHC fills.

call this second case "consumption" of the short circuit). A summary of the context of generation or healing of short circuits is illustrated in Figure 5. This shows that discharges and magnet ramps play an important role both in the generation and in the healing of short circuits in GEM foils. A detailed study of the effects of ramping the CMS magnet on the operation of GE1/1 detectors is reported in [7].

5. Detector efficiency

In 2024 the HV applied to the detectors was tuned chamber by chamber, with values of HV working point I_{eq} in the range $685 - 700\ \mu$A. This was done to obtain the highest possible muon detection efficiency, while still maintaining a low discharge rate. In addition, the configuration of

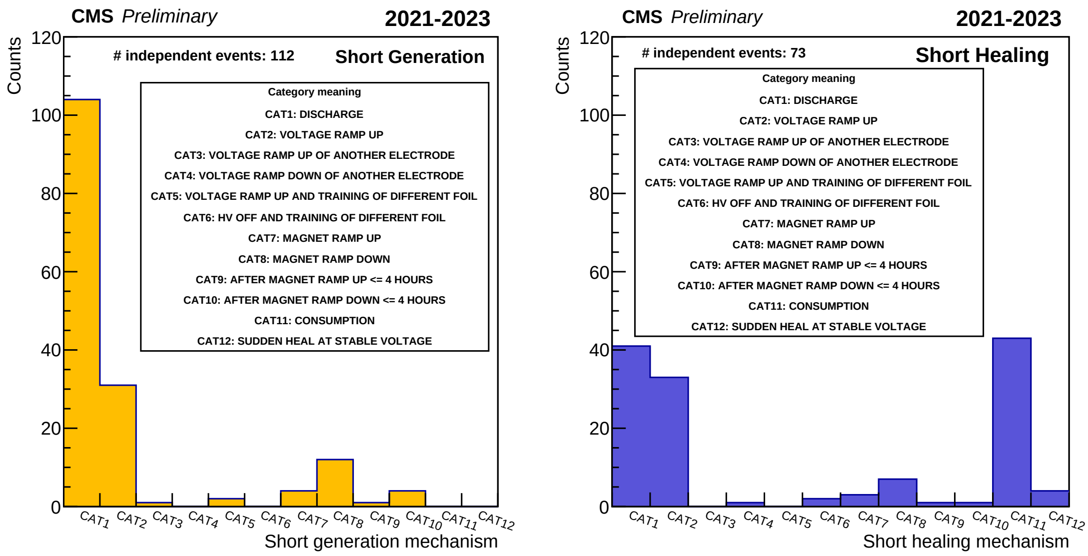

Figure 5: Context of generation or healing of short circuits in GE1/1 GEM foils (2021-2023). Several categories reported on the X-axis can be involved in a generation or healing event. For example: if a short circuit is generated with a discharge (CAT1) and during a voltage ramp up (CAT2), both CAT1 and CAT2 are filled.

the front end electronics (VFAT3 chips [9]) was also tuned increasing the gain of the preamplifier from 8.6 mV/fC (low gain) to 48 mV/fC (high gain). The use of Constant Fraction Discriminator (CFD) was tested, respect to the usage of a simple comparator with a fixed voltage threshold (referred to as ARM mode). The CFD outputs a digital signal with fixed time, independently on the input signal amplitude. The results of this optimization are shown in Figure 6, achieving an average efficiency $\sim 94\%$.

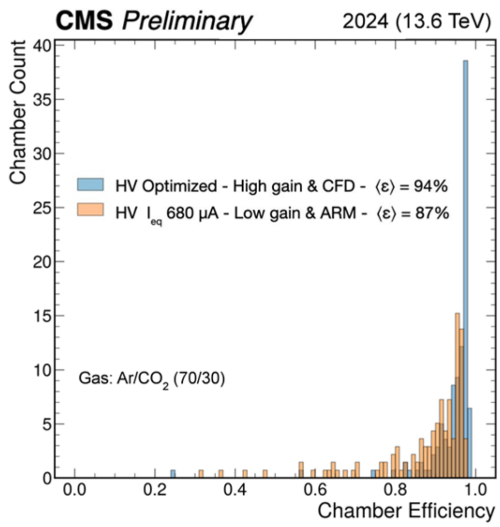

Figure 6: Efficiency of GE1/1 chambers before (orange) and after (blue) the optimization of the HV working point and of the front-end electronics configuration.

6. Conclusion

The GE1/1 chambers were successfully operated during Run 3 in the presence of the LHC beam. The average chamber efficiency achieved in 2024 was 94% when operating the detectors in a range of voltage configurations with $I_{eq} = 685 - 700\ \mu$A. The GE1/1 operation provided useful feedback for understanding the stability of the detectors vs. the occurrence of discharges in presence of the LHC beam. The analysis of generation and healing of short circuits in GEM foils has allowed improvements in the operation of the detectors and gave hints for a thorough ongoing investigation in the manufacturing process.

Acknowledgments

We gratefully acknowledge support from FRS-FNRS (Belgium), FWO-Flanders (Belgium), BSF-MES (Bulgaria), MOST and NSFC (China), BMBF (Germany), DAE (India), DST (India), INFN (Italy), NRF (Korea), and DOE (USA).

References

[1] CMS Collaboration, *The CMS experiment at the CERN LHC,* JINST 3 (2008) S08004, doi:10.1088/1748-0221/3/08/S08004

[2] CMS Collaboration, *Development of the CMS detector for the CERN LHC Run 3,* JINST 19 (2024) P05064, doi:10.1088/1748-0221/19/05/P05064

[3] F. Sauli, *The Gas Electron Multiplier (GEM): operating principles and applications,* Nucl. Inst. Meth. A 805 (2016) 2, https://doi.org/10.1016/j.nima.2015.07.060.

[4] A. Colaleo et al., *CMS Technical Design Report for the Muon Endcap GEM Upgrade,* CERN-LHCC-2015-012, CMS-TDR-013, 2015, https://cds.cern.ch/record/2021453.

[5] M. Abbas, et al., *Quality control of mass-produced GEM detectors for the CMS GE1/1 muon upgrade.* Nucl. Inst. Meth. A 1034 (2022): 166716, https://doi.org/10.1016/j.nima.2022.166716.

[6] CAEN website, "A1515B", https://www.caen.it/products/a1515b/

[7] M. Abbas, et al., *Impact of magnetic field on the stability of the CMS GE1/1 GEM detector operation*, JINST **18** (2023) no.11, P11029 doi: 10.1088/1748-0221/18/11/P11029

[8] S. Calzaferri [CMS Muon], *Analysis of discharge events in the CMS GE1/1 GEM detectors in presence of LHC beam*, JINST **19** (2024) no.02, C02003 doi:10.1088/1748-0221/19/02/C02003

[9] P. Aspell et al. *VFAT3: A Trigger and Tracking Front-end ASIC for the Binary Readout of Gaseous and Silicon Sensors*, 2018 IEEE Nuclear Science Symposium and Medical Imaging Conference Proceedings (NSS/MIC), Sydney, NSW, Australia, 2018, pp. 1-8, doi:10.1109/NSSMIC.2018.8824655